Entropy maximization in the force network ensemble for granular solids

Entropy Maximization in the Force Network Ensemble for Granular Solids

Brian P. Tighe,[1] Adrianne R. T. van Eerd,[2] and Thijs J. H. Vlugt[3]

[1]*Instituut-Lorentz, Universiteit Leiden, Postbus 9506, 2300 RA Leiden, The Netherlands*
[2]*Condensed Matter and Interfaces, Debye Institute for NanoMaterials Science, Utrecht University, P.O. Box 80.000, 3508 TA Utrecht, The Netherlands*
[3]*Delft University of Technology, Process & Energy Laboratory, Leeghwaterstraat 44, 2628 CA Delft, The Netherlands*

(Received 25 March 2008; published 12 June 2008)

A long-standing issue in the area of granular media is the tail of the force distribution, in particular, whether this is exponential, Gaussian, or even some other form. Here we resolve the issue for the case of the force network ensemble in two dimensions. We demonstrate that conservation of the total area of a reciprocal tiling, a direct consequence of local force balance, is crucial for predicting the local stress distribution. Maximizing entropy while conserving the tiling area and total pressure leads to a distribution of local pressures with a generically Gaussian tail that is in excellent agreement with numerics, both with and without friction and for two different contact networks.

DOI: 10.1103/PhysRevLett.100.238001 PACS numbers: 45.70.Cc, 05.40.−a, 46.65.+g

In a granular system the interactions among individual grains are dissipative [1], so that an undriven system eventually jams into a static, mechanically stable configuration [2]. There are typically many jammed states consistent with a given set of macroscopic constraints, e.g., fixed grain number and fixed pressure or volume. A granular packing can move from one jammed configuration to another only under externally imposed fluctuations such as shaking or tapping, because grains are too massive to rearrange thermally [1]. Despite this nonequilibrium nature, Edwards proposed that the methods of equilibrium statistical mechanics might describe many material properties of jammed media [3]. A successful statistical mechanics of jammed systems would represent an important theoretical handle on the physics of granular media. It would permit the calculation of grain scale statistical properties, e.g., volumes [4] or stresses [5–8], from a small number of global constraints. More ambitiously, it would reproduce the complex behavior of granular media in terms of well-defined internal variables.

In this Letter we derive an analytic expression for the probability density $\rho(p)$ of pressures on individual grains in the bulk, which characterizes the strikingly heterogeneous force networks observed in granular solids [9]. We work within the force network ensemble of Snoeijer *et al.* [10] and confirm our results with highly accurate numerics. The force network ensemble comprises all balanced force configurations with a fixed global stress tensor $\langle\hat{\sigma}\rangle$ [11] on a fixed hyperstatic contact network (see below). The ensemble is both a minimal model for the statistics of local stresses and a basic test for any statistical mechanical theory of stress states in granular systems.

There is as yet no clear consensus on the form of the distribution of local stresses in granular media. Of particular interest is the large-stress tail, which early experiments found to be exponential when measured on the boundary [12]. More recent measurements in the bulk [13], along with numerics [14], find distributions that bend downward on a semilogarithmic plot, suggesting faster than exponential decay. A number of proposed theories exploit an analogy to the microcanonical ensemble to arrive at a Boltzmann-like exponential tail [5–7]. These theories should in principle apply to the force network ensemble, but numerical simulations tailor-made to accurately sample large contact forces unambiguously show a Gaussian tail in the force network ensemble in two dimensions [15]. As the present statistical mechanics approaches fail to describe simple models like the force network ensemble, they must be missing an important ingredient. We argue that local force balance is absolutely crucial to describe the correct stress statistics. In particular, we show that the pressure distribution in the force network ensemble directly follows from entropy maximization, but only when it respects a conserved quantity overlooked in previous theories. This conserved quantity follows from force balance at the grain scale, and leads to excellent agreement with numerics for both small and large forces.

Force network ensemble.—Snoeijer's ensemble comprises all "force networks", i.e., sets of noncohesive contact forces on a fixed granular contact network, for which all N grains are in static force and torque balance [e.g., Fig. 1(a)]. For packings with more than a critical number of contacts per grain z_c, termed hyperstatic, there exist many balanced force networks. $z_c = 4$ (3) for frictionless (frictional) 2D packings of disks [10]. All force networks on a contact network with the same $\langle\hat{\sigma}\rangle$ and local force and torque balance can be sampled uniformly by a series of Monte Carlo moves, termed "wheel moves" [15,16]. Figure 1(b) gives an example. In the ensemble each force network has an equal *a priori* probability (a flat measure), in the spirit of the Edwards ensemble [3]. We illustrate our approach in the case of the periodic frictionless triangular lattice of circular grains before expanding to frictional packings and different contact networks.

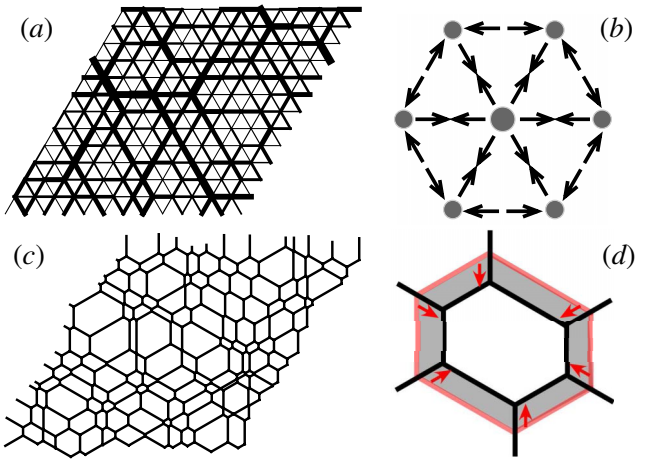

FIG. 1 (color online). A force network (a) on the periodic frictionless triangular lattice. Edges represent contact forces; larger forces are thicker. (b) A wheel move. Arrows represent changes to the forces on each grain. (c) The reciprocal tiling corresponding to (a). Larger forces map to longer lines. (d) A move in the tiling. Shaded area is being exchanged among tiles.

As the global stress tensor $\langle\hat{\sigma}\rangle$ is fixed, the extensive pressure in the system $\mathcal{P} = \sum_i p_i$ is conserved. The sum runs over all grains and $p_i = \mathrm{Tr}\hat{\sigma}_i/2$ is the pressure on grain i. We restrict ourselves to isotropic states, $\langle\hat{\sigma}\rangle \sim \mathbb{1}$, so that $\mathcal{P}$ fully characterizes $\langle\hat{\sigma}\rangle$.

Every force network, regardless of its (dis)ordering, coordination number z, or friction coefficient μ, has a corresponding reciprocal tiling [17]. The systems in Figs. 1(a) and 1(c) are a real and reciprocal pair; each grain corresponds to a tile. Each face of the tile corresponds to one of the grain's contact forces. The face is oriented at a $\pi/2$ rotation to the force $\boldsymbol{f}$, and its length is proportional to $|\boldsymbol{f}|$. Because the grain is in static force balance, the faces form a loop enclosing the tile [18]. By Newton's third law, the tiles fit together with no gaps.

Specifying the boundary forces on a packing establishes the boundaries of its corresponding tiling, and hence the tiling's total area. Fixing $\langle\hat{\sigma}\rangle$ in a periodic system has the same effect. Rearrangements of bulk forces, i.e., the wheel moves, correspond to local exchanges of area among tiles. The total tiling area is unaltered by wheel moves, and therefore the area $\mathcal{A} = \sum_i a_i$ is conserved. The sum runs over all tiles and a_i is the area of tile i [19]. The conservation of $\mathcal{A}$ can be seen explicitly for the frictionless triangular lattice in Fig. 1(d). Area conservation is a global constraint that results from imposing local force balance. It holds for arbitrary force balanced packings in 2D with fixed $\langle\hat{\sigma}\rangle$ or boundary forces. It plays a crucial role in determining the statistics of local stresses.

We scale the grain diameter in the triangular lattice such that the pressure on a grain is the sum of its $z = 6$ normal forces. The perimeter of a tile is then equal to the pressure on the corresponding grain, making pressure a convenient measure of local stress. Though the force distribution $\rho(f)$ is more commonly studied, we expect $\rho(p)$ and $\rho(f)$ to have similar tails.

Entropy maximization.—Armed with the insight that the force network ensemble involves two conserved quantities, $\mathcal{P}$ and $\mathcal{A}$, we explore their implications for the statistics of local stresses. While previous work has incorporated the conservation of $\mathcal{P}$ or its equivalent, the conservation of $\mathcal{A}$ has heretofore been overlooked. We will show that the conservation of $\mathcal{A}$ has a dramatic effect on the force network statistics.

We calculate the probability density $\rho(p)$ by maximizing entropy while conserving $\mathcal{P}$ and $\mathcal{A}$. Each force network corresponds to a set of pressures $\{p_i\}$, $i = 1 \ldots N$. We define $P(p)\omega(p)dp$ as the probability of finding a pressure p in the interval $[p, p + \omega(p)dp)$, where $\omega(p)$ is the density of states for pressures. The entropy S is the logarithm of the number of ways of constructing force networks with pressures $\{p_i\}$ consistent with $P(p)$. In the thermodynamic limit [6]

$$S = -\int_0^\infty (P(p)\ln P(p))\omega(p)dp. \tag{1}$$

The experimentally accessible probability density $\rho(p)$ is related to $P(p)$ by $\rho(p)dp = P(p)\omega(p)dp$.

Weighting all force networks equally does not correspond to a flat measure on the pressures, i.e., $\omega(p) \neq$ const. The contact forces $\{\mathbf{f}_i\}$ on a grain, $i = 1 \ldots z$, can be taken as coordinates of its state space. We demand that a grain explore only the regions of the space corresponding to force and torque balanced, noncohesive forces. We assume that, subject to these constraints and prior to imposing entropy maximization, the grain is equally likely to be in any of its allowed states; this amounts to neglecting correlations with neighboring grains [20]. The result is a density of states that goes as $\omega(p) \propto p^\nu$. The value of ν depends on the grain's coordination number and the friction coefficient. For the frictionless triangular lattice, $\nu = z - 3$.

The entropy is maximized subject to conservation of $\mathcal{P}$ and $\mathcal{A}$, as well as normalization of $\rho(p)$. This leads to

$$\begin{aligned} 1 &= \int_0^\infty \rho(p)dp, \\ \langle p\rangle &= \mathcal{P}/N = \int_0^\infty p\rho(p)dp, \\ \text{and} \quad \langle a\rangle &= \mathcal{A}/N = \int_0^\infty \langle a(p)\rangle\rho(p)dp. \end{aligned} \tag{2}$$

$\langle a(p)\rangle = \int a\rho(a|p)da$ is the average area of a tile with perimeter p; $\rho(a|p)$ is the conditional probability a tile has area a given perimeter p. Maximizing the entropy subject to Eqs. (2) using Lagrange multipliers yields

$$\rho(p) = Z^{-1}p^\nu \exp(-\alpha p - \gamma\langle a(p)\rangle). \tag{3}$$

Without the constraint on tiling area we would have $\gamma = 0$ and an exponential tail: Incorporating local force balance

by means of the area constraint has qualitatively changed the form of the distribution. Z, α, and γ are determined by substituting Eq. (3) in Eqs. (2). For frictionless systems a scaling argument shows that $\langle a(p)\rangle$ is quadratic in the thermodynamic limit [21]; we write $\langle a(p)\rangle = c\langle a\rangle \times (p/\langle p\rangle)^2$ and determine c from numerics. Thus the probability density $\rho(p)$ has a generically Gaussian tail, as was shown numerically for $\rho(f)$ [15].

We employ umbrella sampling [15] on a periodic frictionless triangular lattice with $N = 1840$ to numerically determine $\rho(p)$. From the sampled $\langle a(p)\rangle$, shown in Fig. 2(a), we extract $c \approx 0.89$. Figures 2(b)–2(d) compare the corresponding probability density of Eq. (3) to numerics. Theory and numerics are in excellent agreement, even for $\rho(p)$ as low as 10^{-8}. The slight discrepancies at high p can be attributed to finite size effects and spatial correlations: due to force balance, neighbors of high p grains are themselves more likely to be at high p. Thus large pressures are less entropically favorable than suggested by neglecting correlations.

Frictional lattices.—We now consider frictional triangular ($z = 6$) and square ($z = 4$) lattices. A system with friction coefficient μ permits contact forces with both normal component n and tangential component $t \leq \mu n$. The pressure p remains the sum of normal forces on a grain. Friction has two important consequences. The first is that $\langle a(p)\rangle$ is not strictly quadratic. Friction permits tiles with area $a < 0$, which occurs when tile faces overlap. Nevertheless, on dimensional grounds we still expect $\langle a(p)\rangle \sim p^2$ for large p. In numerics, deviations from a quadratic form increase with μ, but for all frictional systems we have studied quadratic scaling holds for $p \gtrsim \langle p\rangle$. Hence Eq. (3) still yields Gaussian tails. Secondly, we find that friction increases spatial correlations [20]. Consequently, as in Ref. [7], we coarse-grain and study clusters of $m = 7$ (9) grains and $k = 30$ (24) contacts on the triangular (square) lattice. The frictional clusters have exponent $\nu = 2k - 3m - 1$ in their density of states. We find $\langle a(p)\rangle$ for a cluster deviates much less from quadratic behavior than its single-grain counterpart.

Lacking the exact form of $\langle a(p)\rangle$ for frictional systems, we determine the Lagrange multipliers satisfying Eqs. (2) using the numerically sampled $\langle a(p)\rangle$. Theory and numerics are again in excellent agreement, as seen in Fig. 3.

Infinite friction.—As the Lagrange multiplier γ tends towards zero with increasing μ [Figs. 3(b) and 3(d), insets], we investigate the limit $\mu \to \infty$. For finite friction and circular grains, normal and tangential forces are coupled through the force balance constraints on each grain and the Coulomb constraint on each force. In the infinite friction limit the Coulomb constraint has no effect. For the triangular lattice there are three distinct contacts per grain, and it is possible to choose tangential forces $\{t_i\}$ to balance forces and torques for any normal forces $\{n_i\}$. The only constraints on the $\{n_i\}$ are positivity, $n_i > 0$, and fixed $\mathcal{P}$. This leads directly to a Boltzmann distribution

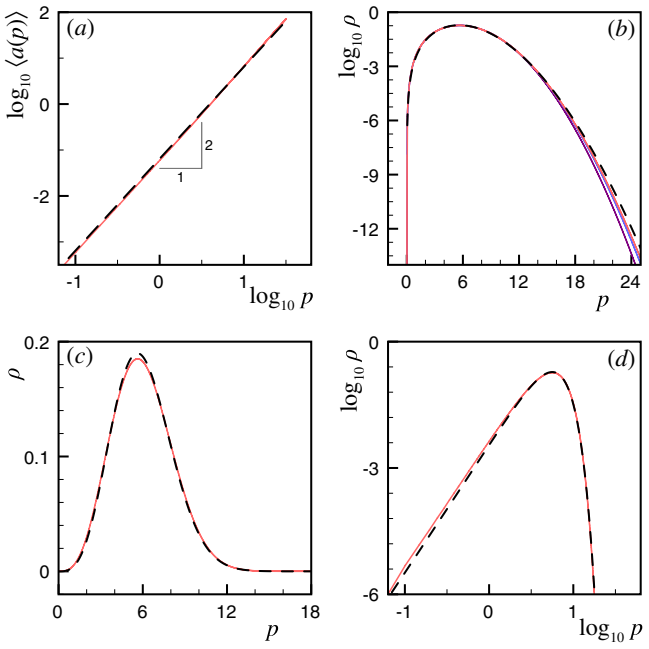

FIG. 2 (color online). (a) Fitted (dashed) and numerical (solid) average area of a tile with perimeter p. (b)–(d) Theoretical (dashed) and numerical (solid) pressure probability distributions for the frictionless triangular lattice with $N = 1840$. The additional numerical curves in (b) are from $N = 460$ and 115.

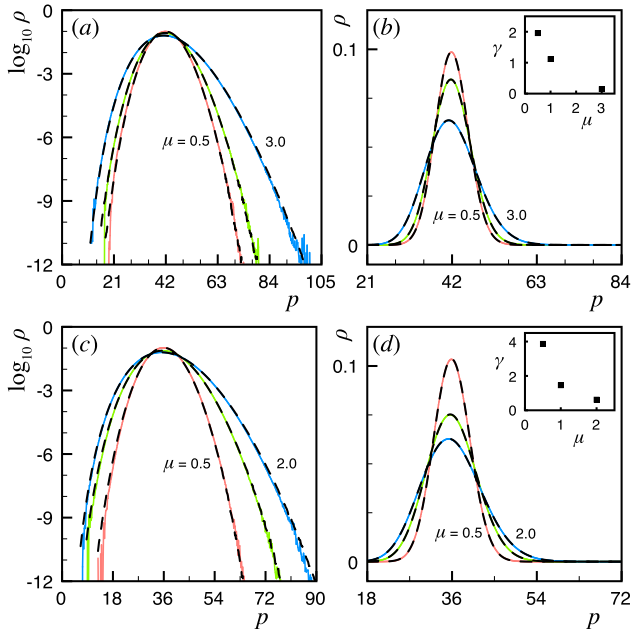

FIG. 3 (color online). (a),(b) Theoretical (dashed) and numerical (solid) pressure probability distributions for 7-grain clusters in the frictional triangular lattice with $\mu = 0.1$, 0.5, 1.0, and 3.0. (c),(d) Pressure distributions for 9-grain clusters in the frictional square lattice with $\mu = 0.5$, 1.0, and 2.0. (b),(d) (inset) γ of Eq. (3) for various friction coefficients μ.

$\rho(n) = \langle n \rangle^{-1} \exp(-n/\langle n \rangle)$ with $\langle n \rangle = \mathcal{P}/zN$. In contrast, for systems with $z - z_c < 3$, such as the square lattice, the normal and tangential forces remain strongly coupled through force balance even for infinite friction. We have confirmed numerically that in the infinite friction limit the Boltzmann distribution holds for the triangular lattice, and that the normal force and pressure distributions in the square lattice remain Gaussian.

Boundary forces.—To this point we have imposed a flat measure on periodic force networks. We have also numerically investigated the frictionless triangular lattice with a boundary subjected to a flat measure on the boundary forces [22]. This produces by prescription an exponential boundary force distribution, reminiscent of experiment [12]. Nevertheless, we find that the force and pressure distributions on grains at least six layers from the boundary have Gaussian tails. This simple example demonstrates that a boundary distribution may not provide direct information about the bulk distribution.

Conclusion.—We have derived an analytic expression for the pressure distribution in the 2D force network ensemble and found excellent agreement with numerics. Distinct from previous studies, we incorporate two conserved quantities, a total pressure and a reciprocal tiling area. The latter is a necessary consequence of local force balance, and we conclude that it is crucial to understanding stress statistics. As a result, large stresses obey Gaussian statistics. This observation is robust to changes in contact network (including disordered networks [15]), finite friction coefficient, and imposed measure.

We have not addressed the distribution at the unjamming transition, which could have a signature in the local stress statistics. Isostatic ($z = z_c$) packings cannot be studied within the force network ensemble. Similarly, our results are restricted to two dimensions. A naïve extension of the reciprocal tiling to 3D suggests $\rho(p) \sim e^{-p^\delta}$ with $\delta = 3/2$, while numerics find $\delta \approx 1.7 \pm 0.1$ [15] within the force network ensemble. The discrepancy may be the result of stronger spatial correlations than in 2D, where coarse graining suffices, or it may signal new physics.

Importantly, along with recent experiments [9,13], our results give serious cause to doubt that exponential statistics are a generic property of jammed granular matter. At the very least, more work is needed to distinguish bulk and boundary phenomena and to clarify why measured boundary forces show exponential statistics.

We thank W. Ellenbroek, Z. Zeravcic, M. van Hecke, and W. van Saarloos for helpful conversations. B. P. T. acknowledges support from the physics foundation FOM and the hospitality of the Aspen Center for Physics, where part of this work was done.

[1] H. M. Jaeger, S. R. Nagel, and R. P. Behringer, Rev. Mod. Phys. **68**, 1259 (1996).
[2] A. J. Liu and S. R. Nagel, Nature (London) **396**, 21 (1998).
[3] S. F. Edwards and R. B. S. Oakeshott, Physica (Amsterdam) **157A**, 1080 (1989).
[4] T. Aste *et al.*, Europhys. Lett. **79**, 24003 (2007); R. Blumenfeld and S. F. Edwards, Phys. Rev. Lett. **90**, 114303 (2003).
[5] S. N. Coppersmith *et al.*, Phys. Rev. E **53**, 4673 (1996); P. Evesque, Poudres et grains **9**, 13 (1999); N. P. Kruyt and L. Rothenburg, Int. J. Solids Struct. **39**, 571 (2002); K. Bagi, Granular Matter **5**, 45 (2003).
[6] J. D. Goddard, Int. J. Solids Struct. **41**, 5851 (2004).
[7] S. Henkes, C. S. O'Hern, and B. Chakraborty, Phys. Rev. Lett. **99**, 038002 (2007).
[8] S. H. Chan and A. H. W. Ngan, Mech. Mater. **37**, 493 (2005); P. T. Metzger, Phys. Rev. E **77**, 011307 (2008).
[9] T. Majmudar and R. P. Behringer, Nature (London) **435**, 1079 (2005).
[10] J. H. Snoeijer *et al.*, Phys. Rev. Lett. **92**, 054302 (2004); J. H. Snoeijer *et al.*, Phys. Rev. E **70**, 061306 (2004).
[11] $\sigma_{\alpha\beta} = \sum_{i,j} f_\alpha^{(i,j)} r_\beta^{(i,j)}/2V$. The sum runs over all contacting grain pairs (i, j) in volume V. $\mathbf{f}^{(i,j)}$ is the force from j on i and $\mathbf{r}^{(i,j)}$ is the vector between their centers.
[12] C. H. Liu *et al.*, Science **269**, 513 (1995); D. M. Mueth, H. M. Jaeger, and S. R. Nagel, Phys. Rev. E **57**, 3164 (1998); G. Løvoll, K. J. Måløy, and E. G. Flekkøy, Phys. Rev. E **60**, 5872 (1999); D. L. Blair *et al.*, Phys. Rev. E **63**, 041304 (2001); J. M. Erikson *et al.*, Phys. Rev. E **66**, 040301(R) (2002); E. I. Corwin, H. M. Jaeger, and S. R. Nagel, Nature (London) **435**, 1075 (2005).
[13] J. Brujić *et al.*, Physica (Amsterdam) **327A**, 201 (2003); J. Zhou *et al.*, Science **312**, 1631 (2006).
[14] F. Radjai *et al.*, Phys. Rev. Lett. **77**, 274 (1996); C. S. O'Hern *et al.*, Phys. Rev. Lett. **86**, 111 (2001); A. V. Tkachenko and T. A. Witten, Phys. Rev. E **62**, 2510 (2000); L. E. Silbert, G. S. Grest, and J. W. Landry, Phys. Rev. E **66**, 061303 (2002).
[15] A. R. T. van Eerd *et al.*, Phys. Rev. E **75**, 060302(R) (2007).
[16] B. P. Tighe *et al.*, Phys. Rev. E **72**, 031306 (2005).
[17] J. C. Maxwell, Philos. Mag. **27**, 250 (1864); G. de Josselin de Jong and A. Verruijt, Cah. Gr. Franc. Rhéol. **2**, 73 (1969).
[18] Upon rotation by $-\pi/2$, the vertices of the tiling are the loop forces of R. C. Ball and R. Blumenfeld, Phys. Rev. Lett. **88**, 115505 (2002).
[19] $a_i = \frac{1}{2}\hat{z} \cdot \sum_{j=1}^{z-2} \sum_{k=j+1}^{z-1} (\mathbf{f}^{(i,j)} \times \mathbf{f}^{(i,k)})$. The indices j and k number the z neighbors of grain i in a right-hand fashion. The unit vector $\hat{z} = \hat{x} \times \hat{y}$ points out of the plane.
[20] The structure factor $S(q) = \langle |p_{\mathbf{q}}|^2 \rangle$ is nearly flat for the frictionless triangular lattice, indicating weak spatial correlations. As μ is increased, $S(q)$ develops an increasingly negative slope, corresponding to more correlated stresses.
[21] Any single-grain state can be transformed into a new one by multiplying its forces by $\lambda > 0$. This scales the perimeter (area) of the corresponding tile by λ (λ^2). Therefore $\rho(a|p) = \lambda^2 \rho(\lambda^2 a|\lambda p)$. Since for frictionless systems $a \geq 0$, it follows that $\langle a(p) \rangle \propto p^2$.
[22] R. Blumenfeld, in *Granular and Complex Materials*, Lecture Notes in Complex Systems Vol. 8, edited by T. Aste, A. Tordesillas, and T. D. Matteo (World Scientific, Singapore, 2007).